

Strength of Correlations in electron and hole doped cuprates

Cédric Weber,¹ Kristjan Haule,¹ and Gabriel Kotliar¹

¹*Department of Physics, Rutgers University, Piscataway, NJ 08854, USA*

High temperature superconductivity was achieved by introducing holes in a parent compound consisting of copper oxide layers separated by spacer layers. Realizations of this phenomena has been achieved in multiple crystal structures and has been the subject of numerous investigations and extensive controversy. In a small number of copper oxide based materials, it is possible to dope the parent compound with electrons [1–3], and their physical properties are bearing some similarities but also significant differences from the hole doped counterparts. For example, in the electron doped materials the antiferromagnetic phase is much more robust than the superconducting phase, while the normal state has a resistivity with a quadratic temperature dependence which is expected in normal metals rather than the linear temperature dependence observed in the hole doped systems. Here, we use a recently developed first principles method, to study the electron doped cuprates and elucidate the deep physical reasons why their behavior is so different than the hole doped materials. The crystal structure of the electron doped materials, characterized by a lack of oxygen in the apical position, results in a parent compound which is a Slater insulator. Namely, a material where the insulating behavior is the result of the presence of magnetic long range order. This is in sharp contrast with the hole doped materials, where the parent compound is a Mott charge transfer insulator, namely a material which is insulating due to the strong electronic correlations but not the magnetic order. We study the evolution of the angle resolved photoemission spectra and the optical properties of the normal state of the electron doped cuprates as a function of doping, clarifying how their unique position close to, but below the metal to charge transfer insulator transition, accounts for their surprising differences from the hole doped cuprates.

We study the prototypical electron doped compound $\text{Nd}_{2-x}\text{Ce}_x\text{CuO}_4$ (NCCO). This is a single-layer material and therefore we compare it to $\text{La}_{2-x}\text{Sr}_x\text{CuO}_4$ (LSCO), a single layer hole doped material in the related T structure. We use a realistic theoretical approach, e.g. the Local Density Approximation combined with the Dynamical Mean Field Theory (LDA+DMFT) [5, 6], and focus on intermediate energy quantities. The results for the electronic spectral functions $A(\omega) = -1/\pi\text{Im}G(\omega)$

of NCCO are shown in Fig. 1. The DMFT equations have two solutions shown in panels **a,b**. The first one is non-magnetic and the second is antiferromagnetically ordered. Notice that the ordered solution, which is stable up to temperature 1400 K, has a charge transfer gap of 1.2eV. When comparing to experiment, it is important to keep in mind that two dimensional compounds are not able to sustain infinite-range magnetic order at a finite temperature. Therefore, the Neel temperature within DMFT should be interpreted as the temperature below which the magnetic correlations become long but remain finite. This temperature can be much higher than the actual Neel temperature of the material, which is controlled by the magnetic exchange between the two dimensional copper oxide layers; and vanishes for a well separated copper oxide planes. DMFT also allow us to investigate the underlying paramagnetic solution, which describes a material in the absence of long range magnetic order. This solution is metallic, and hence the magnetic long range order is responsible for the insulating nature of the compound, as surmised by Slater [8]. It is worth noting that the oxygen orbitals carry no magnetic moment because of the polarization with the two copper neighbors, which have the opposite moments.

In Fig. 1c we resolve the low energy part of panel **b** in momentum space. We find two dispersive coherent peaks separated by the charge transfer gap. In Fig. 1d we resolve the low energy part of panel **b** in orbital space. We find that the occupied and empty states have mostly copper d character with significant oxygen p admixture. The top of the lower band occurs at $(\pi/2, \pi/2)$, while the bottom of upper band appears at $M = (\pi, 0)$, therefore the gap is indirect (see yellow arrow in panel **c**). Those two bands can also be obtained in the simpler Hartree Fock approximation, though the size of the gap is overestimated in a static mean-field.

In Figs. 1e and **f** we show the electronic structure at 10% electron doping. The compound is still magnetic. Some aspects of the doped electronic structure can be understood in terms of the Hartree Fock rigid band picture, the holes appear first in the $M = (\pi, 0)$ point, there are additional narrow quasiparticle states close to but below the Fermi level. The two peak structure of the low energy quasiparticles is clearly seen in the orbital resolved angle integrated spectra of Fig.1 **f**.

Notice also the presence of the pseudogap around $(\pi/2, \pi/2)$, that is a signature of the presence of magnetic long range order, and is also observed in experiments [7] (Fig. 1g, right panel), and compares well to our theoretical calculations (Fig. 1g, left panel). The pseudo-gap

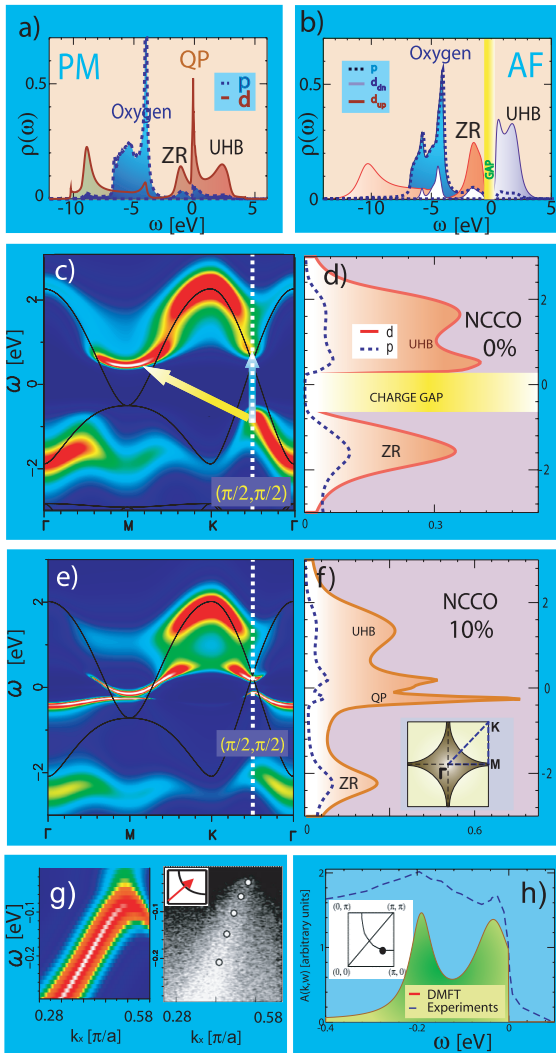


FIG. 1: Density of electronic states in NCCO : (Colors online) Spectral function of NCCO a) nonmagnetic and b) magnetic) at zero doping in the extended energy range. There is a gap of 1.2eV when magnetism is allowed. We clearly observe the presence of the lower (upper) Hubbard bands LHB (UHB), and of a quasi-particle peak in the non-magnetic compound (QP). Frequency dependant spectral weight $A(k,w)$ along $\Gamma - M - K - \Gamma$ obtained by LDA+DMFT at c) integer-filling and e) 10% electron doping (NCCO). The partial density of states of the d and p orbitals are shown on the right panels d) and f). The lines in c) and e) are the LDA rigid bands, plotted in the folded Brillouin Zone, for comparison with DMFT. The corresponding integrated weight is plotted in d) and f). g) side by side comparison of $A(k,w)$, along the path $\Gamma - K$ as depicted in the inset, obtained theoretically (left side) and experimentally from Ref. [7] (right side) at 13% doping. h) comparison of $A(w)$ for a fixed k point $k = (3\pi/4, \pi/4)$ (shown in the inset) obtained theoretically (lower curve) and experimentally from Ref. [7] (upper curve).

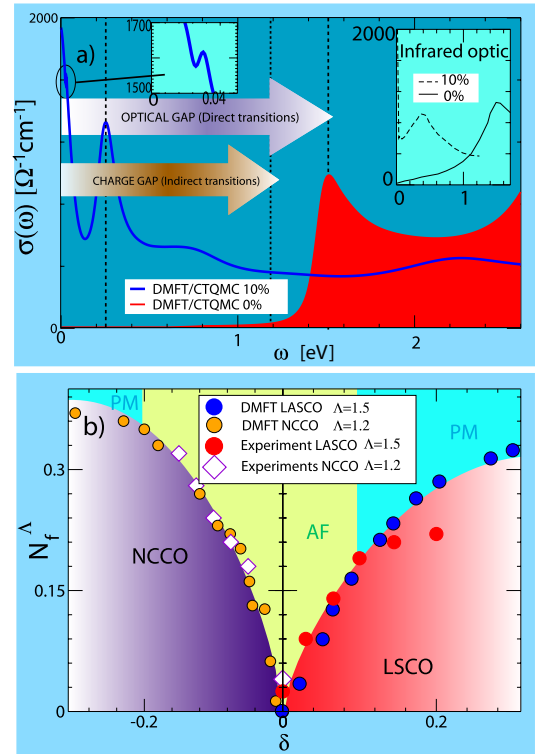


FIG. 2: Optical properties of NCCO : (Colors online) a) Theoretical optical conductivity in $\Omega^{-1}cm^{-1}$ for NCCO doped with charge carriers concentration at integer filling (red curve) and at 10 percent doping (blue curve). At integer-filling, the system is gapped and we observe an optical gap of about 1.5eV, that is larger than the charge gap $\approx 1.2eV$. The left inset is a magnifying glass on the data. For comparison we also show (right inset) the optical conductivity obtained by infrared optics [9]. b) We show the dimensionless integrated optical conductivity N_{eff} for LDA+DMFT done on LSCO and NCCO, obtained with a cutoff $\Lambda = 1.2$ ($\Lambda = 1.5$) for NCCO (LSCO). Experimental data for LSCO [10] (red circles) and NCCO [11] (open diamonds) are shown.

closes in the paramagnetic compound. In Fig. 1h, we also show the spectral weight resolved in frequency for a fixed $k = (3\pi/4, \pi/4)$ point (lower curve). We emphasize the ability of DMFT to resolve the multiple peak structure recently measured in experiments [7] (Fig. 1h upper curve), that cannot be described in a mean-field picture like Hartree Fock.

We now turn to the theoretical optical conductivity, displayed in Fig 2a, which is in good qualitative agreement with the experimental results reproduced in the right inset of Fig 2a. The undoped compound has a sharp onset at an energy of the order of 1.5 eV which we

interpret as the direct gap (slightly larger than the charge transfer gap in Fig. 1d and a tail resulting from indirect transitions. Doping introduces several new features. The $1.5eV$ optical peak loses weight which is transferred to lower energy in the form of a Drude peak and a mid infrared peak at $\omega \approx 0.2eV$.

This peak can be explained in our theory by the presence of magnetism, that leads to a reconstruction of the quasi-particle band structure as shown in Fig. 1e). in agreement with Ref. [12], and additionally our study allow to connect this peak with the spectral weight below the Fermi energy at the $M = (\pi, 0)$ point.

Finally, the optical conductivity display a peak in the magnetic solution at a much lower frequency $\omega \approx 0.03eV$ (see left inset of Fig. 2a), which is connected to the pseudo-gap at $\mathbf{k} = (\pi/2, \pi/2)$, and is also observed in experiments [11].

To quantify the rate of the redistribution of optical spectral weight, is useful to consider the effective electron number per Cu atom defined by $N_{eff}^\Lambda = \frac{2m_e V}{h\pi e^2} \int_0^\Lambda \sigma'(\omega) d\omega$, where m_e is the free electron mass, and V is the cell Volume containing one formula unit. N_{eff} is proportional to the number of electrons involved in the optical excitations up to the cutoff Λ . Our results for (electron doped) NCCO are displayed in the left hand side of Fig. 2b and are compared to experimental data taken from Ref. [11]. Notice a favorable agreement between the theory and experiment, for which the use of the realistic electronic structure is essential. In Fig.2b (right) we also show our theoretical optical spectral weight for a prototypical hole doped cuprate (LSCO), computed in Ref. [4], which is a Mott type insulator, and we compare it to experimental data [10]. The results for a Slater type insulator NCCO and Mott type insulator LSCO are very similar, hence we can conclude that the optical spectral weight is not a precise measure of the strength of correlations.

In a Slater picture, the onset of antiferromagnetism reduces the Coulomb correlations (double occupancy) at the expense of the kinetic energy. The opposite is true in a Mott insulator. Consequently, in a Slater insulator the kinetic energy becomes less negative as the temperature decreases while the opposite happens in a Mott insulator. The kinetic energy as a function of temperature is readily available in the theory and is displayed in Fig 3a (top panel).

A closely related quantity N_{eff} is experimentally accessible and has been measured for this compound. In Fig 3b (top panel) we plot both the experimental [11] and our theoretical data, which are in very good agreement. Experiments of Ref. [11] confirm that N_{eff} is closely related to minus the kinetic energy. It has therefore already been confirmed that NCCO is below the metal to charge transfer insulator transition in experiments.

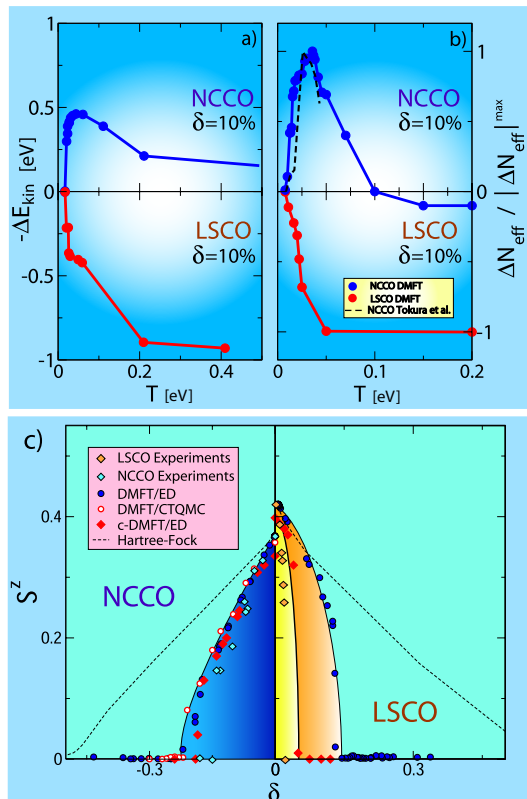


FIG. 3: **Kinetic energy and magnetic phase diagram:** (Colors online) a) Theoretical kinetic energy variation $-\Delta E_{kin} = -E_{kin}(T) + E_{kin}(89^\circ K)$ of the electron (top panel) and the hole (bottom panel) doped compounds with respect to temperature. b) Normalized variation of N_{eff} , $\Delta N_{eff} = N_{eff}(T) - N_{eff}(89^\circ K)$ of the electron (top panel) and the hole (bottom panel) doped compounds with respect to temperature. The dashed line are extracted from experiments done on NCCO [11]. c) Mean-value of the staggered magnetization obtained for LSCO and NCCO by both single site (DMFT) and cluster DMFT (c-DMFT). Experimental values $M(\delta)/M_0$ ($M_0 = M(\delta = 0)$) for NCCO [13] and LSCO [14] are also shown, and for comparison with DMFT, we assume $M_0 = M_{DMFT}(\delta = 0)$, where M_{DMFT} is the magnetic moment at 0 doping obtained by single site DMFT. We also show the magnetization obtained in the static hartree-fock approximation (dashed line) are shown for comparison.

In Fig. 3a (bottom panel) we also plot the temperature dependence of the kinetic energy and N_{eff} for the hole doped Mott insulator (LSCO). We find the opposite trend compared to the lightly electron doped NCCO compound, confirming that LSCO is a doped Mott insulator.

Finally, in order to check the validity of our single site DMFT approach, we computed the magnetic phase diagram and magnetic moment within the single site and

two-site cluster DMFT (see Fig. 3.c). Our data for NCCO are displayed on the left side of Fig. 3.c) and are compared to experimental data from Ref.[13]. The agreement is very good for both approaches, hence justifying the use of the single sited DMFT approach.

The right site of Fig. 3.c) displays theoretical and experimental magnetic moment[14] for hole doped LSCO. We found significant difference in the region of stability of the magnetic state between the single site and cluster DMFT ($\delta < 10\%$), hence the dynamical short range correlations - absent in single site approach - are very important for LSCO in the underdoped regime, but not for NCCO.

We also carried out the Hartree-Fock calculation, and we found that in this static approach the magnetization vanishes only at unrealistic large doping $\delta \approx 50\%$ for both NCCO and LSCO (dashed line in Fig. 3.c), which points towards the important role of dynamic correlations at finite electron and hole doping.

Our theory sheds light on many puzzling observations. It was noticed within the context of the one band model that the doping dependent Hubbard interaction was needed to reproduce experiments [15]. In our view, this is a description, within a one band model, of the rapid metallization process in a Slater-like insulator. A realistic LDA+DMFT treatment of the multiband Hamiltonian does not require doping dependent interactions. The strong sensitivity of the electronic properties to magnetism, which results from the fact that the physics of NCCO is closer to that of a Slater insulator than of a Mott insulator, gives rise to additional experimental predictions. We expect that at high temperatures (of the order of the DMFT mean field temperatures) there should be appreciable transfer of spectral weight from high energies to low energies with decreasing temperature, as the magnetic correlations are weakend, and a substantial decrease of the Mott Hubbard gap and the weights in the Hubbard bands. This can be checked by extending transport and photoemission studies in lightly doped electron doped cuprates from 600 to 1100 K.

In materials where the strength of the interaction is below the critical value need to produce a Mott insulating state, the effective interactions can renormalize down, allowing superconductivity and magnetism to coexist microscopically rather than exclude each other. This coexistence provides a good description of the Raman scattering of the electron doped superconductors [19]. Finally, in some NCCO films the parent compound was found to be metallic. It would be interesting to study the magnetic properties of these materials to see if this metallicity correlates with a substantial decrease of the magnetic correlations [20].

We thank A.M. Tremblay, D. Basov, D. G. Hawthorn, G. A. Sawatzky for discussions and sharing their insights and experimental data. Numerous discussions with A. Georges, A. Amaricci, J. C. Domenge and A. Millis are

gratefully acknowledged. Adriano Amaricci shared his density matrix renormalization group code and Jean-Christophe Dommene shared his exact diagonalization code. K.H was supported by Grant NSF NFS DMR-0746395 and Alfred P. Sloan fellowship. G.K. was supported by NSF DMR-0906943, and C.W. was supported by the Swiss National Foundation for Science (SNFS).

METHOD

The LDA calculation was carried out with the PWSCF package [21], which employs a plane-wave basis set and ultrasoft pseudopotentials [22]. We downfold to a three band model, containing copper $d_{x^2-y^2}$ and two oxygen p_σ orbitals using the maximally localized Wannier functions method (MLWF) [23]. The results of this procedure can be summarized in the following three band Hamiltonian:

$$\mathcal{H} = \sum_{ij\sigma, (\alpha, \beta) \in (p_x, p_y, d_{x^2-y^2})} t_{ij}^{\alpha\beta} c_{i\alpha\sigma}^\dagger c_{j\beta\sigma} + \epsilon_p \hat{N}_p + (\epsilon_d - E^{dc}) \hat{N}_d + U_d \sum_i \hat{n}_{id\uparrow} \hat{n}_{id\downarrow} \quad (1)$$

where i and j label the CuO_2 unit cells of the lattice, and $t_{ij}^{\alpha\beta}$ are the hopping matrix elements, and ϵ_d , ϵ_p are the on-site energies of the d and p orbitals. The onsite Coulomb repulsion U on the $d_{x^2-y^2}$ orbital was fixed to $U_d = 8eV$. Finally, we note that $\epsilon_d - \epsilon_p$ plays the role of an effective onsite repulsion U in a Hubbard model picture. The LDA+DMFT method, accounts for the correlations which are included in both LDA and DMFT by a double counting correction to the d -orbital energy, E_{dc} which amounts to a shift of the relative positions of the d and p levels which we take to be doping independent and $E_{dc} = 4.8eV$ ($3.12eV$) for NCCO (LSCO). The LDA downfolded hopping parameters are presented in the online material. The Green function of the three band model is given by:

$$\mathbf{G}_{\mathbf{k}}(i\omega_n) = (i\omega_n + \mu - \mathbf{H}_{\mathbf{k}} - \mathbf{\Sigma}(i\omega_n))^{-1}, \quad (2)$$

where $\mathbf{H}_{\mathbf{k}}$ is the Fourier transform of the \mathcal{H}_t in Eq. (1) and $\mathbf{\Sigma}$ is the DMFT self-energy matrix, which is assumed to be local, and nonzero only for the d orbital. The self energy in Eq. (2) is obtained by solving an Anderson impurity model subject to the DMFT self-consistency condition

$$\frac{1}{i\omega - E_{imp} - \Sigma(i\omega) - \Delta(i\omega)} = \frac{1}{N_k} \sum_{\mathbf{k} \in BZ} G_{\mathbf{k}}^{dd}(i\omega), \quad (3)$$

where the sum runs on the first Brillouin Zone (BZ). The self-energy $\mathbf{\Sigma}$ is obtained by solving an Anderson impurity using the continuous time quantum Monte Carlo impurity solver [24, 25] (CTQMC) and the exact diagonalization solver [5] (ED). Calculations have been carried

out at temperature $T = 89^\circ K$, when not specified in the text. Finally, the optical conductivity is given by

$$\sigma'(\omega) = \frac{1}{N_k} \sum_{\sigma \mathbf{k}} \frac{\pi e^2}{\hbar c} \int dx \frac{f(x - \omega) - f(x)}{\omega} \times \text{Tr}(\hat{\rho}_{\mathbf{k}\sigma}(x - \omega) \mathbf{v}_{\mathbf{k}} \hat{\rho}_{\mathbf{k}\sigma}(x) \mathbf{v}_{\mathbf{k}}), \quad (4)$$

where c is the interlayer distance, the density matrix $\hat{\rho}$ is $\hat{\rho}_{\mathbf{k}\sigma}(x) = \frac{1}{2\pi i} (\mathbf{G}_{\mathbf{k}\sigma}^\dagger(x) - \mathbf{G}_{\mathbf{k}\sigma}(x))$, and the bare vertex is obtained by following the steps of Ref [26].

-
- [1] N.P. Armitage et al., Phys. Rev. B. **68**, 064517 (2003).
 - [2] H. Takagi et al., Phys. Rev. Lett. **62**, 1197(1989).
 - [3] Y. Tokura and A. Fujimori, Phys. Rev. B **39**, 9704 (1989)
 - [4] C. Weber, K. Haule, and G. Kotliar, Phys. Rev. B. **78**, 134519 (2008)
 - [5] A. Georges et al., Rev. Mod. Phys., **68**, 0034 (1996)
 - [6] K Held et al., J. Phys.: Condens. Matter, **20**, 064202 (2008)

- [7] H. Matsui et al., Journal of Physics and Chemistry of Solids, **67** 249 (2006).
- [8] J. C. Slater, *Quantum theory of molecules and solids*, (McGraw-Hill, New-York, 1974), Vol. 4.
- [9] T. Xiang et al., Phys. Rev. B **79**, 014524 (2009).
- [10] S. Uchida *et al.*, Phys. Rev. B **43**, 7942 (1991).
- [11] Y. Onose et al., Phys. Rev. B. **69**, 024504 (2004).
- [12] A. Zimmers et al, Europhys. Lett. **70**, pp. 225-231 (2005).
- [13] P. K. Mang *et al.*, Phys. Rev. Lett. **93**, 027002 (2004).
- [14] F. Borsa et al., Phys. Rev. B. **52**, 7334 (1995).
- [15] B. Kyung et al., Phys. Rev. Lett. **93**, 147004 (2004)
- [16] O. Matsumoto et al., Phys. Rev. B, **79**, 100508 (2009)
- [17] Guo-meng Zhao, condmat/0907.2011
- [18] Y. Qingshan et al., Phys. Rev. B **72**, 054504 (2005)
- [19] B. Stadlober et al., Phys. Rev. Lett. **74**, 4911 (1995).
- [20] J.-P. Ismer et al., arXiv: 0907.1296.
- [21] PWSCF in Quantum Espresso Package (2007) URL <http://www.pwscf.org/>.
- [22] D. Vanderbilt, Phys. Rev. B **41**, 7892 (1990).
- [23] I. Souza, N. Marzari, and D. Vanderbilt, Phys. Rev. B **65**, 035109 (2001).
- [24] K. Haule and G. Kotliar, Phys. Rev. B **76**, 104509 (2007).
- [25] P. Werner *et al.*, Phys. Rev. Lett. **97**, 076405 (2006).
- [26] Jan M. Tomczak, Eur. Phys. Lett. **86**, 37004 (2009).